HEP

Science and Engineering Research Council
Rutherford Appleton Laboratory
Chilton DIDCOT Oxon OX11 0QX

RAL-93-014

Phenomenological Constraints on the Flavour Asymmetry of the Nucleon Sea

A D Martin W J Stirling and R G Roberts

rch 1993

DTP/93/12
RAL-93-014
March 1993

Phenomenological constraints on the flavour asymmetry of the nucleon sea

A.D. Martin and W.J. Stirling

Department of Physics, University of Durham
Durham DH1 3LE, England

and

R.G. Roberts

Rutherford Appleton Laboratory,
Chilton, Didcot OX11 0QX, England

Abstract

We study the possible flavour asymmetry, $\bar{u} \neq \bar{d}$, of the light quark sea distributions of the proton. We discuss the information that is at present available from data on deep-inelastic lepton-nucleon scattering and from Drell-Yan production on various nuclear targets. We show that the ratio of dilepton yields on hydrogen and deuterium targets is very sensitive to $\bar{u} - \bar{d}$.

The increased precision of deep inelastic lepton-nucleon scattering data has considerably improved our knowledge of the parton distributions of the proton. Until recently all global structure function analyses assumed that the light quark sea distributions satisfied the equality $\bar{u} = \bar{d}$. However, motivated by the improvement of the data, particularly at small x, and by the consequences for the Gottfried sum rule, analyses [1,2,3] have been performed with $\bar{u} \neq \bar{d}$. Here we wish to explore how large an inequality the available data can tolerate and to see how well future experiments can pin down $\bar{u} - \bar{d}$.

Valuable insight into the problem is obtained by expressing (to leading order) the observed muon and neutrino deep inelastic structure functions in terms of the parton densities

$$F_2^{\mu p} - F_2^{\mu n} = \tfrac{1}{3}x(u + \bar{u} - d - \bar{d}) \quad (1)$$

$$\tfrac{1}{2}(F_2^{\mu p} + F_2^{\mu n}) = \tfrac{5}{18}x(u + \bar{u} + d + \bar{d} + \tfrac{4}{5}s) \quad (2)$$

$$F_2^{\nu N} = F_2^{\bar{\nu} N} = x(u + \bar{u} + d + \bar{d} + 2s) \quad (3)$$

$$\tfrac{1}{2}x(F_3^{\nu N} + F_3^{\bar{\nu} N}) = x(u - \bar{u} + d - \bar{d})\,, \quad (4)$$

where N is an isoscalar nuclear target, and where we have included the s quark, but neglected the (small) c quark, contribution. These four observables determine four combinations of parton densities, which we can take to be $u + \bar{u}$, $d + \bar{d}$, $\bar{u} + \bar{d}$ and s. In other words data at a given x, Q^2 cannot verify whether $\bar{u} = \bar{d}$ or not.

The above discussion is very simplistic because in practice we must (i) include the next-to-leading $O(\alpha_s)$ contributions, which require knowledge of the gluon distribution, (ii) allow for possible adjustments in the overall relative normalisation of the data sets, (iii) include the heavy target corrections of the neutrino data, and (iv) include screening corrections to allow $F_2^{\mu n}$ to be obtained from deuterium data. Assuming that this has all been done correctly, we compare in Fig. 1 the parton distributions at $Q^2 = 20$ GeV^2 from the two most recent global analyses [2,3]. If we make a detailed comparison at, say, $x = 0.15$ then we see significant differences between $u, d, \bar{u}, \bar{d}$ from the two sets of partons. For CTEQ [3] we have $\bar{d} \simeq 2\bar{u}$, while for MRS [2] we have $\bar{d} \simeq \bar{u}$.[1] However this difference is compensated by u(CTEQ) $> u$(MRS) and d(CTEQ) $< d$(MRS) so that the observable combinations $u+\bar{u}$, $d+\bar{d}$

[1]This difference is a consequence of the flexible (and independent) parametrizations of the $\bar{u}, \bar{d}, s$ distributions allowed in the CTEQ analysis [3]. However the most dramatic difference between the CTEQ and MRS distributions is in the behaviour of the s quark distribution (the dash-dot curves on Fig. 1). The freely parametrized CTEQ s distribution becomes relatively large at small x to accommodate the $F_2^{\nu N}$ data for $x \lesssim 0.1$. On the other hand MRS [1,2] adopted a less flexible parametrization, with $s = \frac{1}{4}(\bar{u} + \bar{d})$ at $Q^2 = 4$ GeV^2, and allowed for uncertainties in the heavy target corrections to the neutrino data; the (factor of 2) suppression of the s quark distribution was chosen so as to be in better accord with dimuon production in deep inelastic neutrino scattering [4].

and $\bar{u}+\bar{d}$ remain essentially the same in both analyses, as indeed they should be for values of x where accurate data exist. So, as mentioned above, without additional input, the structure function data on their own do not test $\bar{u} \neq \bar{d}$.

The motivation for $\bar{u} \neq \bar{d}$ comes from the NMC measurement [5]

$$\int_{0.004}^{0.8} \frac{dx}{x}(F_2^{\mu p} - F_2^{\mu n}) \;=\; 0.227 \pm 0.007(\text{stat.}) \pm 0.014(\text{sys.}) \qquad (5)$$

at $Q^2 = 4$ GeV^2, as compared to the Gottfried sum rule

$$\begin{aligned} I_{GSR} \;=\; \int_0^1 \frac{dx}{x}(F_2^{\mu p} - F_2^{\mu n}) \;&=\; \frac{1}{3}\int_0^1 dx(u_v - d_v) + \frac{2}{3}\int_0^1 dx(\bar{u} - \bar{d}) \\ &=\; \frac{1}{3} \qquad \text{if} \qquad \bar{u} = \bar{d}\,, \end{aligned} \qquad (6)$$

where here u and d have been expressed as the sum of valence and sea distributions, *e.g.* $u = u_v + u_s$ and $\bar{u} = u_s$. A straightforward comparison of (5) and (6) implies that $\bar{d} > \bar{u}$, and indeed from the lack of Regge $f_2 - a_2$ exchange degeneracy we expect

$$\bar{d} - \bar{u} \;=\; Ax^{-\alpha_R}(1-x)^{\eta_S} \qquad (7)$$

with the small x behaviour governed by the Regge (meson trajectory) intercept $\alpha_R \simeq 0.5$. In the global analyses of refs. [1,2] we parametrized $\bar{d} - \bar{u}$ in this way and found $I_{GSR} \simeq 0.24 - 0.26$. However it is possible to achieve an equally acceptable global fit of all the structure function data with $\bar{u} = \bar{d}$ (and hence $I_{GSR} = \frac{1}{3}$), albeit with a contrived small x behaviour of the valence distributions [1].

Fig. 2 shows the ingredients of the Gottfried sum rule for various sets of parton distributions with $\bar{u} \neq \bar{d}$. The central part of the figure, which shows $F_2^{\mu p} - F_2^{\mu n}$ on a logarithmic x scale, is a visual display of the integrand of the sum rule at $Q^2 = 7$ GeV^2. The data are from NMC [6]. The top part of the figure shows the accumulated contribution to the sum rule as we integrate down from $x = 1$; thus the limiting values of the curves as $x \to 0$ give I_{GSR} of (6). The central curves in the shaded bands are obtained from the MRS(D$_0'$) partons with $\bar{d} - \bar{u}$ parametrized at $Q^2 = 4$ GeV^2 as in (7); these partons give $I_{GSR} = 0.256$ [2].

In order to explore the allowed variations in the *shape* of the x behaviour of $\bar{d} - \bar{u}$ we have repeated the global analysis of ref. [2] with the difference having the extended parametrization

$$\bar{d} - \bar{u} \;=\; Ax^{-\alpha_R}(1-x)^{\eta_S}(1 + \gamma x + \delta x^2), \qquad (8)$$

with A chosen to maintain the normalisation $I_{GSR} = 0.256$. First we set $\delta = 0$. We find that we can maintain the quality of the fit to the data, that was achieved by the D$_0'$ fit of ref. [2], provided that γ lies in the range $-8 \lesssim \gamma \lesssim 32$. These extreme

"hard" and "soft" versions of $\bar{d}-\bar{u}$ of D_0' correspond to the boundary curves of the shaded regions shown in Fig. 2. We may thus regard the shaded region as a first qualitative estimate of the uncertainty in $\bar{d}-\bar{u}$. We see that this range of fits only modifies $F_2^{\mu p}-F_2^{\mu n}$ for $x \lesssim 0.05$; indeed deep-inelastic data impose only a weak constraint on $\bar{d}-\bar{u}$ at larger values of x. For a determination of $\bar{d}-\bar{u}$ at larger x we should compare Drell-Yan production of pp and pn origin. A hint of what may be possible is shown in Fig. 3, which compares Drell-Yan data [7] obtained from a neutron rich (tungsten) target with those from isoscalar (deuterium and carbon) targets. We discuss such Drell-Yan comparisons, in detail, below.

We have also repeated the global analysis of the deep inelastic data with $\delta \neq 0$ in the parametrization (8) of $\bar{d}-\bar{u}$, in an attempt to reproduce the qualitative trend of the Drell-Yan data of Fig. 3. The predictions of a fit with $\gamma = -60$, $\delta = 300$ are shown by the dashed curves on Figs. 2 and 3. These have a radically different shape and, in fact, the quality of the fit to the deep inelastic data diminishes; we regard this as an example of extreme behaviour of $\bar{d}-\bar{u}$. For completeness we show by dot-dashed curves the predictions of the CTEQ1M analysis, which is in the spirit of the D_0' fit but with $\bar{u}, \bar{d}, s$ much more freely parametrized. We see a dramatically different behaviour at small x; indeed $F_2^{\mu p}-F_2^{\mu n}$ becomes negative for $x < 0.006$ and as a result the value of I_{GSR} is well below 0.2.

The distributions shown in the lower part of Fig. 2 therefore offer (i) a set of conservative variations of $\bar{d}-\bar{u}$ of the D_0' fit which are consistent with all the deep inelastic data, together with (ii) two examples of unusual (but interesting) behaviour which arise if the sea distributions are more freely parametrized.

The Drell-Yan process provides a complementary method of investigating the antiquark content of the nucleon. In leading order, for a proton beam on a nuclear target A,

$$\frac{d^2\sigma}{dM^2 dx_F} = \frac{4\pi\alpha^2}{9M^2 s}\,\frac{1}{x_p + x_A}\,\sum_q e_q^2\,[q(x_p)\bar{q}(x_A) + \bar{q}(x_p)q(x_A)]\,, \qquad (9)$$

with $\tau = M^2/s = x_p x_A$ and $x_F = x_p - x_A$. The crucial point is that a comparison of the cross sections on targets with *different* numbers of protons and neutrons leads directly to information on $\bar{d}-\bar{u}$. Two methods have been suggested. The first [7] relies on the fact that at large x_F the cross section (9) is dominated by the annihilation of u quarks in the proton with $\bar{u}$ quarks in the target. If the latter contains Z protons and $A-Z$ neutrons, then

$$\frac{d^2\sigma}{dM^2 dx_F} \approx \frac{4\pi\alpha^2}{9M^2 s}\,\frac{1}{x_p + x_A}\,\frac{4}{9}\,u(x_p)\frac{1}{A}\{Z\bar{u}(x_A) + (A-Z)\bar{d}(x_A)\}\,. \qquad (10)$$

In particular the ratio of non-isoscalar to isoscalar target cross sections is [7]

$$R_{A/IS}(x) \approx 1 + \left(1 - \frac{2Z}{A}\right) \frac{\bar{d}(x) - \bar{u}(x)}{\bar{d}(x) + \bar{u}(x)}, \tag{11}$$

with $x \equiv x_A$. The ratio for tungsten (with $1 - 2Z/A = 0.195$) to isoscalar targets has recently been measured by the E772 collaboration [7]. A comparison of their data with the predictions of the various parton sets discussed above is shown in Fig. 3. The open circles at small x show the data before a correction for nuclear shadowing is applied [7]. It turns out that the x_F values are largest for the data points at small x, and it is only for these that the approximation (11) is valid. At larger x, the smaller x_F values lead to a contamination of the $u(x_p)\bar{u}(x_A)$ annihilation with the other processes, and a corresponding decrease of the sensitivity to $\bar{d} - \bar{u}$. The shaded band in Fig. 3 again corresponds to the range $\delta = 0$, $-8 < \gamma < 32$ of the $\bar{d} - \bar{u}$ parametrization of (8), evaluated using the full Drell-Yan next-to-leading order cross section. The D_0' prediction (solid line) is roughly in the middle of this band. The S_0' prediction (not shown) has $R \simeq 1$ for small x, falling slightly to $R \simeq 0.99$ at the larger x values. All these predictions are clearly consistent with the measured ratio. Notice that there is perhaps some evidence that $R < 1$ (*i.e.* $\bar{d} < \bar{u}$) for $x \lesssim 0.15$. As mentioned above, it is not difficult to derive a $\bar{d} - \bar{u}$ form which follows this trend, as shown by the dashed line in Fig. 3 which corresponds to $\delta = 300$, $\gamma = -60$, though this parametrization leads to a poorer overall fit to the deep inelastic data. Note also that the CTEQ1M prediction (dot-dashed curve), which has $\bar{d} - \bar{u}$ large and positive for the range of x spanned by the data, appears to be slightly disfavoured.

A much more powerful Drell-Yan measurement is to compare the cross sections on proton and neutron (in practice hydrogen and deuterium) targets [8]. Two such experiments have recently been proposed [9,10]. Fig. 4 shows the next-to-leading order QCD prediction for the asymmetry

$$A_{DY} = \frac{\sigma(pp) - \sigma(pn)}{\sigma(pp) + \sigma(pn)}, \tag{12}$$

where $\sigma \equiv d^2\sigma/dMdy|_{y=0}$, as a function of $\sqrt{\tau}$ at $p_{\rm beam} = 450$ GeV/c, corresponding to the proposed CERN experiment [9].[2] The parton distributions are the same as in Fig. 3. Because $u > d$ in the proton, the asymmetry is positive for sets with $\bar{d} - \bar{u}$ zero or small at large x. The asymmetry is reduced and can even become negative for sets with large $\bar{d} - \bar{u}$, in particular the CTEQ1M set. A measurement of this asymmetry in the $\sqrt{\tau} = 0.1 - 0.3$ range to an accuracy of a few percent will

[2]The predictions for the corresponding Fermilab energy are virtually indistinguishable.

therefore provide a powerful discriminator of the possible behaviours of the $\bar{d} - \bar{u}$ difference. Note also that the sensitivity of the asymmetry (12) to $\bar{d} - \bar{u}$ increases at forward rapidity (equivalently $x_F > 0$): at large y, where $u\bar{u}$ annihilation again dominates, we have simply that $A_{DY} \approx (\bar{u} - \bar{d})/(\bar{u} + \bar{d})$, which is equivalent to (11) with $1 - 2Z/A = 1$.

In conclusion, we find that deep inelastic data do not unambiguously determine $\bar{u}$ and $\bar{d}$. However, if a reasonable behaviour is imposed on $\bar{d} - \bar{u}$ at small x (motivated by a small breaking of meson exchange degeneracy) then the data indicate a small flavour asymmetry with $\bar{d} > \bar{u}$ for $x \lesssim 0.01$. Global fits to data imply that the $\bar{d} > \bar{u}$ inequality persists to larger x, but it is possible to introduce more flexible parametrizations of $\bar{d} - \bar{u}$. We show that a comparison of Drell-Yan production on hydrogen and deuterium targets will provide a good determination of $\bar{d} - \bar{u}$ in the medium x range. Finally, it is worth noting that a small, positive $\bar{d} - \bar{u}$ is a common feature of most model calculations [11,12] of the sea quark flavour asymmetry, in particular those involving mesonic contributions to the deep inelastic structure functions. For example, the Drell-Yan predictions of the chiral quark model of ref. [12] are very similar to those of our standard D_0' fit.

References

[1] A.D. Martin, W.J. Stirling and R.G. Roberts, Phys. Rev. **D47** (1993) 867.

[2] A.D. Martin, W.J. Stirling and R.G. Roberts, RAL preprint-92-078 (1992).

[3] CTEQ collaboration: J. Botts, J. Morfin, J. Owens, J. Qiu, W. Tung and H. Weerts, preprint FERMILAB-PUB-92-371 (1993).

[4] CCFR collaboration: C. Foudas *et al.*, Phys. Rev. Lett. **64** (1990) 1207; S.A. Rabinowitz *et al.*, Phys. Rev. Lett. **70** (1993) 134.

[5] NMC: P. Amaudruz *et al.*, Phys. Rev. Lett. **66** (1991) 2712.

[6] NMC: E.M. Kabuß, Nucl. Phys. (Proc. Supp.) **29A** (1992) 1.

[7] E772 collaboration: P.L. McGaughey *et al.*, Phys. Rev. Lett. **69** (1992) 1726.

[8] S.D. Ellis and W.J. Stirling, Phys. Lett. **256** (1991) 258.

[9] M.C. Abreu *et al.*, "Study of the Isospin Breaking in the Light Quark Sea from the Drell-Yan Process", CERN proposal CERN/SPSLC 92-15 (unpublished).

[10] G.T. Garvey *et al.*, "Measurement of $\bar{d}(x)/\bar{u}(x)$ in the Proton", Fermilab proposal P866 (unpublished).

[11] E.M. Henley and G.A. Miller, Phys. Lett. **251B** (1990) 453.
M. Anselmino and E. Predazzi, Phys. Lett. **254B** (1991) 203.
J. Stern and G. Clément, Phys. Lett. **264B** (1991) 426.
S. Kumano, Phys. Rev. **D43** (1991) 59; **D43** (1991) 3067.
S. Kumano and J.T. Londergan, Phys. Rev. **D44** (1991) 717; **D46** (1992) 457.
A. Signal, A.W. Schreiber and A.W. Thomas, Mod. Phys. Lett. **A6** (1991) 271.
W.-Y.P. Hwang and J. Speth, Phys. Rev. **D46** (1992) 1198.
J. Speth and A. Szczurek, Jülich preprint KFA-IKP-TH-1992-1 (1992).

[12] E.S. Eichten, I. Hinchliffe and C. Quigg, Phys. Rev. **D45** (1992) 2269; preprint FERMILAB-PUB-92-264-T (1992).

Figure Captions

[1] The parton distributions of the proton at $Q^2 = 20$ GeV^2 corresponding to (a) set D'_0 of MRS [2] and to (b) set CTEQ1M of [3] .

[2] The upper plot shows the accumulated contribution to the Gottfried sum rule, (6), as a function of x, the lower limit of integration, which is obtained from sets of partons with differing behaviour of $\bar{d} - \bar{u}$, as shown in the lower plot (for $Q^2 = 7$ GeV^2). The shaded bands contain a family of parton solutions with $\bar{d} - \bar{u}$ given by (8) with $-8 < \gamma < 32$ and $\delta = 0$; the central curves in the bands corresponds to set D'_0 of [2] with $\gamma = 0$. The dashed curves correspond to a fit with $\delta \neq 0$ in (8), and the dot-dashed curves correspond to set CTEQ1M of [3]. The central part of the figure shows the integrand of the Gottfried sum rule, together with NMC data [6] which we have corrected, at small x, for deuteron screening effects.

[3] The ratio of dilepton yields per nucleon from tungsten and isoscalar (deuterium and carbon) targets as a function of x(target). The data are from ref. [7]; the open circles at small x show the ratio before the correction for nuclear shadowing. The curves are the full next-to-leading order QCD predictions using the same parton sets as in Fig. 2. Thus the shaded band corresponds to a range of distributions with $\bar{d} - \bar{u}$ given by (8) with $-8 < \gamma < 32$ and $\delta = 0$; the central curve in the band corresponds to set D'_0 of [2] with $\gamma = 0$. The dashed curve corresponds to a fit with $\delta = 300$, $\gamma = -60$ in (8), while the dot-dashed curve corresponds to set CTEQ1M of [3].

[4] Predictions for the Drell-Yan asymmetry $A_{DY} = (\sigma(pp) - \sigma(pn))/(\sigma(pp) + \sigma(pn))$, where $\sigma \equiv d^2\sigma/dMdy|_{y=0}$, as a function of $\sqrt{\tau} = M/\sqrt{s}$ with $p_{\rm beam} = 450$ GeV/c. The curves are based on next-to-leading order calculations using the same parton distributions as in Fig. 3.

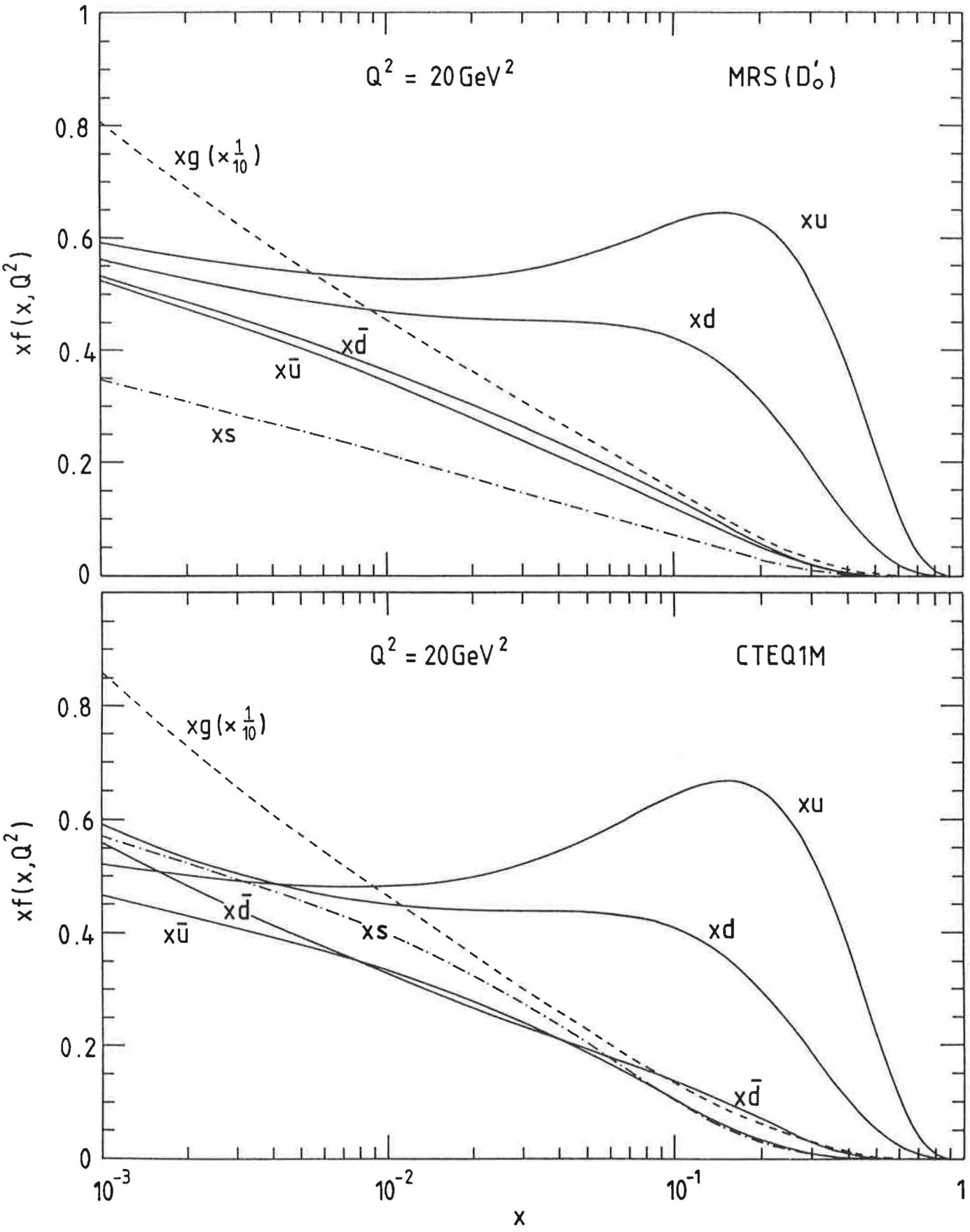
$Q^2 = 20\,GeV^2$
MRS (D_o')
xg ($\times\frac{1}{10}$)
xu
xd
$x\bar{d}$
$x\bar{u}$
xs
$Q^2 = 20\,GeV^2$
CTEQ1M
xg ($\times\frac{1}{10}$)
xu
xd
$x\bar{d}$
$x\bar{u}$
xs
$xf(x,Q^2)$
x
0
0.2
0.4
0.6
0.8
1
10^{-3}
10^{-2}
10^{-1}
1

Fig. 1

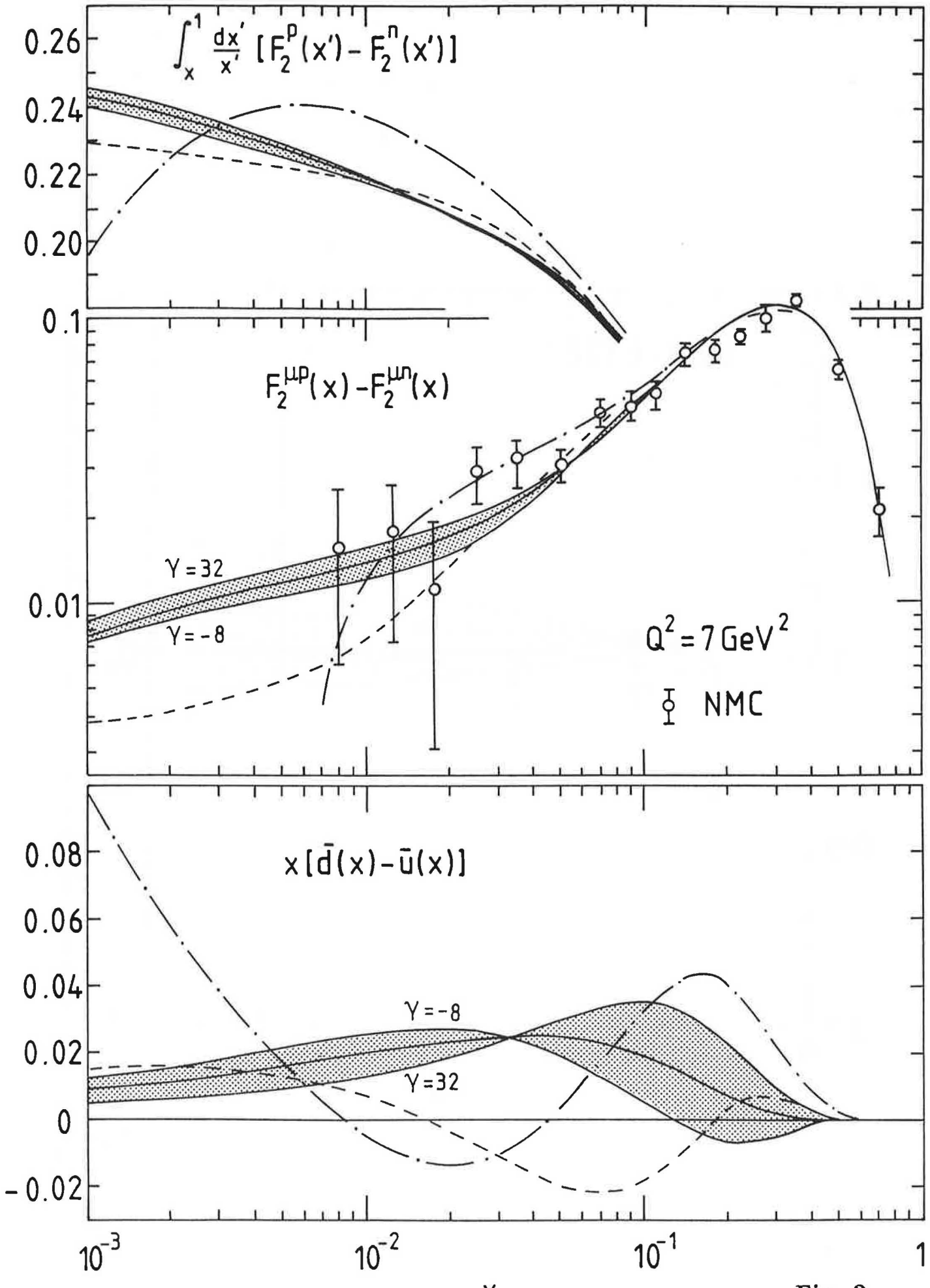
$\int_x^1 \frac{dx'}{x'} [F_2^p(x') - F_2^n(x')]$
0.26
0.24
0.22
0.20
0.1
$F_2^{\mu p}(x) - F_2^{\mu n}(x)$
$\Upsilon = 32$
$\Upsilon = -8$
0.01
$Q^2 = 7\,GeV^2$
NMC
$x[\bar{d}(x) - \bar{u}(x)]$
0.08
0.06
0.04
$\Upsilon = -8$
0.02
$\Upsilon = 32$
0
- 0.02
10^{-3}
10^{-2}
10^{-1}
1
x

Fig. 2

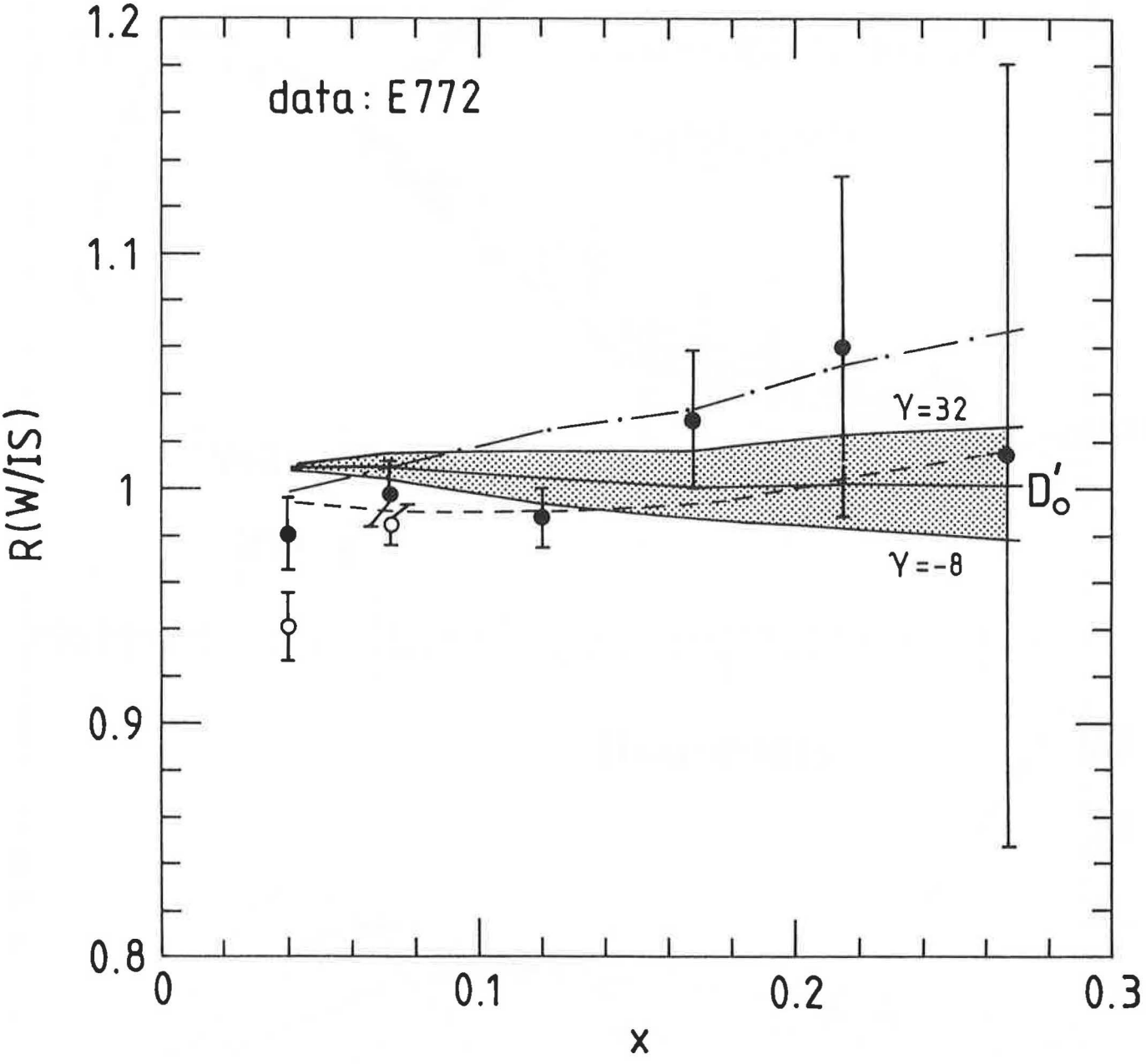

Fig. 3

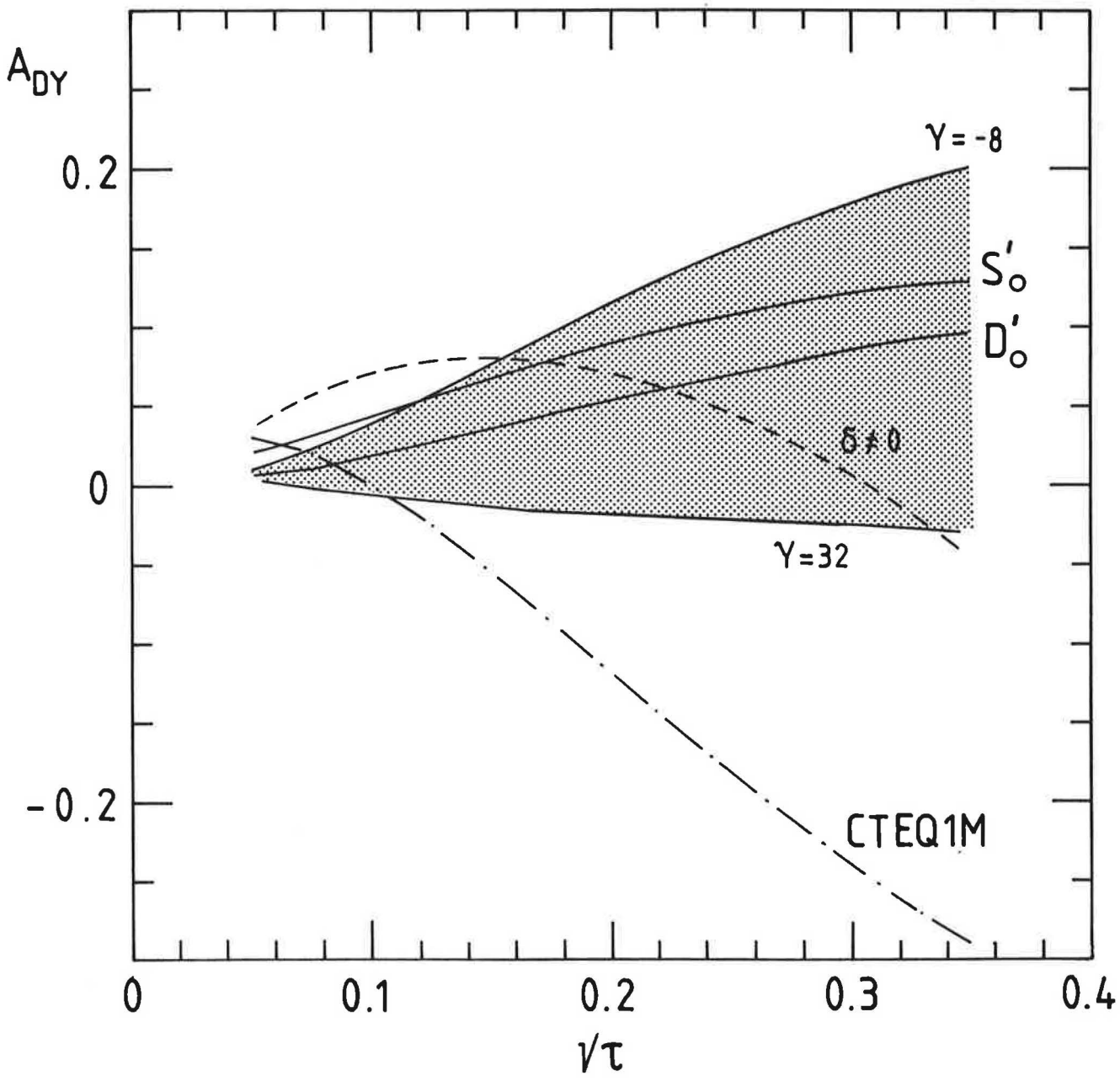

Fig. 4